



NIH Public Access

Author Manuscript

J Neurosci Res. Author manuscript; available in PMC 2009 April 1.

Published in final edited form as:
J Neurosci Res. 2008 April ; 86(5): 992–1006. doi:10.1002/jnr.21561.

Cx29 and Cx32, Two Connexins Expressed by Myelinating Glia, Do Not Interact and Are Functionally Distinct

Meejin Ahn¹, Jonathan Lee¹, Andreas Gustafsson¹, Alan Enriquez¹, Eric Lancaster¹, Jai-Yoon Sul², Philip G. Haydon², David L. Paul³, Yan Huang¹, Charles K. Abrams⁴, and Steven S. Scherer^{1,*}

¹ Department of Neurology, University of Pennsylvania School of Medicine, Philadelphia, Pennsylvania

² Department of Neuroscience, University of Pennsylvania School of Medicine, Philadelphia, Pennsylvania

³ Department of Neurobiology, Harvard Medical School, Boston, Massachusetts

⁴ Department of Neurology, SUNY Downstate Medical Center, Brooklyn, New York

Abstract

In rodents, oligodendrocytes and myelinating Schwann cells express connexin32 (Cx32) and Cx29, which have different localizations in the two cell types. We show here that, in contrast to Cx32, Cx29 does not form gap junction plaques or functional gap junctions in transfected cells. Furthermore, when expressed together, Cx29 and Cx32 are not colocalized and do not coimmunoprecipitate. To determine the structural basis of their divergent behavior, we generated a series of chimeric Cx32-Cx29 proteins by exchanging their intracellular loops and/or their C-terminal cytoplasmic tails. Although some chimerae reach the cell membrane, others appear to be largely localized intracellularly; none form gap junction plaques or functional gap junctions. Substituting the C-terminus or the intracellular loop and the C-terminus of Cx32 with those of Cx29 does not disrupt their colocalization or coimmunoprecipitation with Cx32. Substituting the C-terminus of Cx29 with that of Cx32 does not disrupt the coimmunoprecipitation or the colocalization with Cx29, whereas substituting both the intracellular loop and the C-terminus of Cx32 with those of Cx29 diminishes the coimmunoprecipitation with Cx29. Conversely, the Cx32 chimera that contains the intracellular loop of Cx29 coimmunoprecipitates with Cx29, indicating that the intracellular loop participates in Cx29-Cx29 interactions. These data indicate that homomeric interactions of Cx29 and especially Cx32 largely require other domains: the N-terminus, transmembrane domains, and extracellular loops. Substituting the intracellular loop and/or tail of Cx32 with those of Cx29 appears to prevent Cx32 from forming functional gap junctions.

Keywords

Schwann cells; oligodendrocytes; gap junctions; myelin; mutations

Gap junctions (GJ) allow the intercellular passage of ions and small molecules up to about 1,000 Da and are thought to have diverse functions, including the propagation of electrical signals, metabolic cooperation, growth control, spatial buffering of ions, and cellular

*Correspondence to: Steven S. Scherer, MD, PhD, Department of Neurology, University of Pennsylvania Medical School, Room 464 Stemmler Hall, 36th Street and Hamilton Walk, Philadelphia, PA 19104-6077. E-mail: sscherer@mail.med.upenn.edu.
Yan Huang's current address is State Key Laboratory of Genetic Engineering, Institute of Genetics, School of Life Science, Fudan University, Shanghai, People's Republic of China

Supplementary Material for this article is available online at [http://www.mrw.interscience.wiley.com/suppmat/0360-4012/suppmat/\(www.interscience.wiley.com\).](http://www.mrw.interscience.wiley.com/suppmat/0360-4012/suppmat/(www.interscience.wiley.com).)

differentiation (Bruzzone et al., 1996). Six connexins oligomerize into a hemichannel (or connexon), and two hemichannels on apposing cell membranes form the channel; aggregates of tens to thousands of channels form a GJ plaque. Individual hemichannels can be composed of one (homomeric) or more (heteromeric) type of connexins. Similarly, channels may contain hemichannels with the same (homotypic) or different (heterotypic) connexins. Because more than 20 mammalian connexins have been described (Willecke et al., 2002; they are named according to their predicted molecular mass), there are potentially a large number of different kinds of hemichannels and especially channels.

In rodents, oligodendrocytes and myelinating Schwann cells express connexin32 (Cx32) and Cx29; oligodendrocytes also express Cx47 (Scherer et al., 1995; Altevogt et al., 2002; X. Li et al., 2002, 2004; Nagy et al., 2003a, b; Kleopa et al., 2004; Eiberger et al., 2006; Tang et al., 2006; J. Li et al., 2007). In myelinating Schwann cells, Cx32 is localized mainly to the noncompact myelin of paranodes and incisures. Cx29 is also localized to paranodes and incisures, but, unlike Cx32, Cx29 is expressed prominently on the adaxonal Schwann cell membrane (apposing the axonal membrane), particularly in the juxtaparanodal region. In oligodendrocytes, Cx32 and Cx47 are localized to the cell somata and outer aspects of large myelin sheaths, likely forming heterotypic gap junctions with the astrocytic connexins, Cx30 and Cx47, respectively. In oligodendrocytes, Cx32 is also localized between the layers of the myelin sheath, but these Cx32-containing gap junctions are less conspicuous than those in myelinating Schwann cells. Cx29 is mainly localized to the adaxonal membrane of small myelin sheaths. Because gap junctions are not found between the adaxonal membrane and the axon, it has been speculated that Cx29 forms hemichannels on the adaxonal membrane of oligodendrocytes and myelinating Schwann cells (Kamasawa et al., 2005).

The colocalization of Cx29 and Cx32 in incisures and paranodes in Schwann cells raises the possibility that these connexins interact at these sites, but their lack of colocalization in the adaxonal membrane indicates that the two are targeted differently. We investigated these issues by generating chimeric proteins in which the intracellular loop and/or C-terminal cytoplasmic tail of mouse Cx29 and mouse Cx32 were swapped. We chose these two regions because they are the most divergent portions of connexins (Willecke et al., 2002). These chimerae were expressed with either mouse Cx29 or mouse Cx32 in gap junction-deficient HeLa cells. Cx32 and Cx29 did not physically associate with each other, and substituting the Cx29 tail or the Cx29 loop and tail domains into Cx32 did not affect the ability of these chimerae to associate with Cx32. In contrast, substituting the Cx32 loop into Cx29 diminished its interaction with Cx29 and substituting the Cx29 loop into Cx32 enabled it to interact with Cx29. Thus, the intracellular loop domain is an important regulator of Cx29 but not Cx32 homomeric assembly. In addition, none of the chimeric proteins, nor Cx29 itself, formed gap junction plaques or functional gap junctions. Thus, substituting the intracellular loop and/or tail of Cx32 with those of Cx29 appears to prevent Cx32 from forming functional gap junctions.

MATERIALS AND METHODS

Generation of Cx29/Cx32 Chimerae

The open reading frames of mouse Cx29 and Cx32 were obtained by RT-PCR (Superscript II; Invitrogen, Carlsbad, CA) from mouse brain and liver RNA, respectively, using oligonucleotide primers and Platinum Pfx DNA polymerase. Cx32 inserts were isolated by double digestion with NheI and EcoRI; Cx29 inserts were double digested with NotI and EcoRV. Inserts were ligated into pIRESpuro3 (Clontech, Palo Alto, CA). Following the strategy of Rubin et al. (1992), we generated “megaprimer”s of the intracellular loop (L^{32} ; amino acids 97–127) and tail (T^{32} ; amino acids 209–283) of Cx32, as well as the intracellular loop (L^{29} ; amino acids 97–130) and tail (T^{29} ; amino acids 211–258) of Cx29. In making each megaprimer, we used primer pairs that included an extra 18 bases corresponding to the amino

acid sequence of the six adjacent amino acids of the connexin into which the megaprimer was to be incorporated. Using the QuickChange Mutagenesis Kit (Stratagene, La Jolla, CA), the L³² and T³² megaprimers were added to Cx29 template to generate Cx29L³² and Cx29T³², respectively; the L²⁹ and T²⁹ megaprimers were added to Cx32 template to generate Cx32L²⁹ and Cx32T²⁹, respectively. The L³² megaprimer was added to Cx29T³² template to generate Cx29L³²T³²; the L²⁹ megaprimer was added to Cx32T²⁹ template to generate Cx32L²⁹T²⁹. The resulting PCR products were used to transform DH5 α competent cells, a large-scale plasmid preparation was made from a single colony (Qiagen, Valencia, CA), and the sequence was directly confirmed at the Cell Center at the University of Pennsylvania. The open reading frame of human Cx47 was similarly obtained by RT-PCR of human brain and cloned into pIRESpuro3 (Orthmann-Murphy et al., 2007).

Cell Culture and Transfections

Communication-incompetent HeLa cells (Elfgang et al., 1995) were obtained from Dr. Klaus Willecke. These cells do not show gap junctional intercellular communication by scrape loading or by microinjection of low-molecular-mass tracers (Elfgang et al., 1995), nor do they express Cx29 or Cx32 (see below). COS-7 cells and Neuro2A cells were obtained from the American Type Tissue Collection. Cells were grown in low-glucose Dulbecco's modified Eagle's medium (DMEM) supplemented by 10% fetal bovine serum and antibiotics (100 μ g/ml penicillin/streptomycin) in a humidified atmosphere containing 5% CO₂ at 37°C. For transient transfection, Lipofectamine 2000 (Invitrogen) and either 1 μ g or 4 μ g of plasmid DNA for immunostaining or immunoblotting respectively, were incubated separately in Optimem (Gibco-BRL) for 5 min at room temperature (RT), then combined for another 20 min. When cells were approximately 80% confluent, they were washed with Optimem, then incubated with the combined Lipofectamine/DNA solution for 6 hr at 37°C. After 6 hr, the cells were washed once with HBSS (free of calcium and magnesium) and incubated for 3 days in media at 37°C for 2–3 days, then processed for immunostaining or immunoblotting.

To obtain stably expressing, bulk-selected cells, 1 mg/ml puromycin (Sigma-Aldrich, St. Louis, MO) was added 3 days after transiently transfecting HeLa cells. The cells were maintained in puromycin-supplemented medium, with medium changes every 3–4 days, until colonies with stable growth were obtained. The colonies were admixed after trypsinization and expanded in puromycin for immunocytochemistry and functional testing. To obtain single clones of cells expressing Cx29, single colonies were picked from stably expressing cells grown at low density. Untransfected HeLa cells were also treated with puromycin and did not survive after 2 weeks.

Generation of Antisera Against the Cx32 Cytoplasmic Tail

The nucleotide sequence corresponding to amino acids 237–283 of the C-terminus of Cx32 was amplified by PCR using human Cx32 as the template, primers (5'-cgcggatcccaccgccttcacctgaata-3', and 5'-ccggaaattcgagggttgccctgttatgt-3'), and the Pfu Turbo Polymerase Kit (Stratagene). The PCR product was ligated with the T4 Rapid Ligation Kit (Roche, Indianapolis, IN) into the pGEX-2TK vector (Amersham Biosciences, Uppsala, Sweden), which encodes a glutathione S-transferase moiety. The resulting construct was used to transform DH5 α bacteria, a large-scale plasmid preparation was made from a single colony (Sigma-Aldrich) and analyzed at the Sequencing Core of the University of Pennsylvania. The construct was transformed into BL21 codon + RP Competent Cells (Stratagene); the GST-fusion protein was purified using glutathione-Sepharose beads (Amersham Biosciences), then sent to Covance Research Products (Denver, PA) to develop polyclonal antisera from two rabbits using Freund's adjuvant, with five boosters at 3-week intervals. The preimmune and first, second, third, and terminal bleeds were tested by immunostaining HeLa cells that were transiently transfected to express Cx32, and on unfixed teased fibers from WT mice and *Gjb1*/

cx32 null mice. The preimmune bleed did not stain transfected cells or teased fibers from WT mice, whereas every post-immunization bleed immunostained a proportion of transfected cells, the incisures and paranodes of WT teased fibers, but not teased fibers from *Gjb1/cx32* null mice (data not shown).

Immunocytochemistry

Parental and transiently transfected HeLa, COS-7, and Neuro2A cells, as well as bulk-selected or clonal lines of HeLa cells were grown on coverslips or in slide chambers (Fisher Scientific) until 60% confluent, washed in 1 × PBS, fixed in acetone at -20°C for 10 min, blocked with 5% fish skin gelatin in 1 × PBS containing 0.1% Triton X-100 for 1 hr at RT. The cells were labeled with various combinations of mouse monoclonal antibodies against Cx32 tail (7C6.C7, diluted 1:1; Deschênes et al., 1997), the Cx32 loop (Zymed; diluted 1:500), or “pan-cadherins” (Abcam, Cambridge, MA; diluted 1:500), a goat antiserum against Rab7 (Santa Cruz, Santa Cruz, CA; diluted 1:40), rabbit antisera against the Cx32 loop (Chemicon, Temecula, CA; diluted 1:500), the Cx32 tail (Chemicon; diluted 1:500, or a rabbit antiserum that we generated ourselves; 1:1,000), the Cx29 tail (affinity-purified, diluted 1:10; Altevogt et al., 2002), and a rat monoclonal against GRP94 (Abcam; diluted 1:250), diluted in the same blocking solution and incubated overnight at 4°C. After washing in PBS, the FITC- and/or TRITC-conjugated donkey anti-mouse/rabbit/goat/rat secondary antibodies were added in the same blocking solution and incubated at RT for 1 hr. Coverslips were mounted with Vectashield (Vector, Burlingame, CA), and samples were photographed with a Leica fluorescence microscope with a Hamamatsu digital camera connected to a G5 Mac computer, using the Openlab 2.2 software for deconvolution. Unless otherwise stated, the images were adjusted in Adobe Photoshop (Adobe Systems), so that the entire dynamic range of pixel intensity was used. We confirmed that all of the Cx29 and Cx32 antibodies used in this study immunostained transfected but not untransfected cells as well as PNS and/or CNS myelin sheaths of WT but not of Cx29 and *Gjb1/cx32* null mice, respectively.

For quantification of the pixel overlap of Rab7 and Cx32T²⁹, Cx32L²⁹T²⁹, Cx29, or Cx32, we selected pairs of images from single planes obtained on a confocal microscope, converting each image into an eight-bit black-and-white format. With NIH Image J, we traced the contours of one or two contiguous cells using the polygon tool cursor, then set the threshold such that only the brightest pixels in the Rab7 channel (6.0–6.5% of the total pixels) and Cx29/Cx32 channel (12.0–12.5% of the total pixels) would be included in our analysis. The selected pixels that overlap were used to form a new image (using the “image calculator” function), and their number was determined (using the “particle analysis” function). We compared samples with the Mann-Whitney-Wilcoxon U-test, a nonparametric test for pairwise comparisons.

Scrape Loading

Bulk-selected cells expressing pIRESpuro3, Cx29, Cx32, or one of the Cx29/Cx32 chimerae were grown to confluence on 60-mm plates. The external medium was changed to HBSS (without calcium, magnesium, or phenol red) and 0.1% Lucifer yellow (Sigma-Aldrich) or 2% Neurobiotin (Vector), and a razor blade was used to inscribe many parallel lines on the dish. For Lucifer yellow, the cells were incubated in HBSS (with calcium and magnesium, but no phenol red) after 5 min, imaged using a Nikon Eclipse TE 2000-U microscope with both fluorescence and phase-contrast optics, and photographed with a RTKE Spot camera.

Fluorescence Recovery After Photobleaching

HeLa parental cells and cloned HeLa cells that stably express mouse Cx29 or human Cx47 were grown to confluence in slide chambers. Samples were incubated with fluorescent dye calcein-AM (2.5 µg/ml; Molecular Probes, Eugene, OR) for 30 min at RT and washed with PBS. Fluorescence recovery after photobleaching (FRAP) and confocal fluorescence imaging

was performed on an Olympus BX51 microscope with an attached Prairie confocal scan head (Prairie Technologies, Madison, WI). Ten initial images (5-sec interval between images) were obtained from a region of interest (ROI) to establish the baseline fluorescence intensity of a small group of cells, which was then photobleached using the full power 488-nm laser illumination with the confocal software. After photobleaching, images were continuously acquired every 10 sec for up to 1 hr to monitor fluorescence recovery. The fluorescence intensity of cells distant from the photobleached ROI was subtracted from that of the ROI to correct for photobleaching result from imaging the experiment after photobleaching, but this was negligible (less than 10% bleaching over 30 min). Fluorescence intensities of ROIs were analyzed in Metamorph software (Universal Imaging Corp., West Chester, PA).

Immunoblotting, Biotinylation, and Coimmunoprecipitation

For immunoblotting, 35-mm plates of transiently transfected or bulk-selected HeLa cells were washed twice with Dulbecco's 1 × PBS lacking calcium and magnesium. Cell were lysed by adding 150 µl of ice-cold RIPA buffer (10 mM sodium phosphate, pH 7.0, 150 mM NaCl, 2 mM EDTA, 50 mM sodium fluoride, 1% NP-40, 1% sodium deoxycholate, and 0.1% SDS) to each plate, incubated for 15 min on ice, removed with a cell scraper, and transferred to a microfuge tube. Lysates were spun at 14,000 rpm; then, the supernatants were collected, a cocktail of protease inhibitors was added (Sigma-Aldrich), and the protein concentrations were determined using the Bio-Rad kit (Bio-Rad, Hercules, CA) according to the manufacturer's instructions. For each sample, 80 µg protein lysate was incubated with loading buffer at RT for 5–15 min, loaded onto a 12% SDS-polyacrylamide gel, electrophoresed at 120 V until the dye front left the stacking gel, then increased to 160 V for about 1 hr until the dye front reached the bottom of the gel. Blots were transferred to an Immobilon-polyvinylidene fluoride membrane (Millipore, Billerica, MA) for 75 min using a semidry transfer unit (Bio-Rad). The blots were blocked (5% blotting grade blocker nonfat dry milk and 0.5% Tween-20 in Tris-buffered saline) overnight at 4°C and incubated with various antibodies (diluted in blocking solution) for 24 hr at 4°C: a rabbit antiserum against the C-terminal tail of Cx29 (Altevogt et al., 2002; 1:1,000), a commercially obtained rabbit antiserum against Cx29 (Zymed; 1:10,000), a mouse monoclonal antibody against the cytoplasmic loop of Cx32 (Zymed; 1:500), or a mouse monoclonal antibody against the C-terminal tail of Cx32 (7C6.C7; Deschênes et al., 1997; 1:10). The blots were washed in blocking solution and incubated in peroxidase-coupled donkey antibody against rabbit or mouse IgG (Jackson Immunoresearch, West Grove, PA; diluted 1:10,000) for 1 hr at RT. After washing in blocking solution and Tris-buffered saline containing 0.5% Tween-20, the blots were visualized by enhanced chemiluminescence (Amersham, Piscataway, NJ) according to the manufacturer's protocol.

Cell membrane proteins were biotinylated following the protocol of VanSlyke et al. (2000). Plates (35 mm) of transiently transfected HeLa cells were grown to ~80% confluence at 37°C, placed on a metal plate on ice, incubated with chilled PBS⁺ (PBS plus 1 mM MgCl₂ and 0.5 mM CaCl₂) for 10 min, rinsed three times with PBS⁺, and incubated with 0.5 mg/ml biotin (Pierce, Rockford, IL) on a shaking platform for 30 min at 4°C. The biotinylation medium was removed, and the cells were washed five times with PBS⁺ and 100 mM glycine (pH 7.6), rinsed with PBS⁺, rinsed twice with PBS⁺ plus protease inhibitors (PMSF, pepstatin A, leupeptin, and aprotinin, and incubated in lysis buffer (5 mM Tris/5 mM EDTA/5 mM EGTA, pH 8, plus 0.6% SDS, 15 mM glycine) and protease inhibitors. Cells were removed with a rubber cell scraper, collected with a 1-ml syringe with 22-gauge needle, placed in a microfuge tube, and incubated at RT for 30 min. Cell lysates were passed through a 26-gauge needle three times and diluted with 2.5 volumes of IP dilution buffer (0.1 M NaCl, 20 mM sodium borate, 0.02% NaN₃, 15 mM EDTA, 15 mM EGTA, pH 8.2), so the final ratio of Triton X-100:SDS = 5:1. Tubes were spun at 13,000 rpm in RT for 10 min; the supernatant was transferred to a new microfuge tube; 50 µl of a 50% streptavidin agarose slurry was added to each tube and rotated

overnight at 4°C. The next day, tubes were spun for 2 min at 13,000 rpm at RT; the supernatant was removed and saved (the “unbound fraction”). The streptavidin beads were washed four times with 1 ml IP buffer plus 0.5% Triton X-100:0.1% SDS, vortexed gently, and spun for 2 min at 13,000 rpm in RT. After the fourth wash, the beads were washed with 0.5 ml IP buffer + 0.05% Triton X-100:0.1% SDS, and the beads for two plates were combined. After a 2-min spin at 13,000 rpm at RT, the supernatant was removed, the beads were spun for another 2 min at 13,000 rpm at RT, and the remaining wash buffer was removed from the beads with a 30-gauge needle attached to a 1-cc syringe. Biotinylated proteins were eluted out from the beads by adding loading buffer with 2% β-mercaptoethanol and incubated at 37°C for 5 min (the “bound fraction”). All of the bound fractions and 25 μl of the unbound fractions were run on 10% PAGE-SDS gels and transferred to membranes, which were hybridized with either a rabbit antiserum against the C-terminus of Cx29 (Cx29T; Zymed) or a mouse monoclonal antibody against the C-terminus of Cx32 (Cx32T; 7C6.C7).

For coimmunoprecipitations, 35-mm plates of transiently cotransfected HeLa cells were grown to ~80% confluence at 37°C. Cells were washed twice with PBS and placed on cold metal plates. Cells were lysed by adding 500 μl ice-cold RIPA buffer to each plate, incubated for 15 min on ice, removed with a cell scraper, and transferred to a microfuge tube. Lysates were spun at 14,000 rpm, supernatants were collected, and a cocktail of protease inhibitors was added. Rabbit antiserum (15 μg) against the C-terminus of mCx29 (Zymed) was added to each sample incubated on a rocking platform at 4°C. Protein G agarose (Invitrogen) prewashed with RIPA buffer was added, and the supernatant/antibody/bead mixtures were placed on a rotator overnight at 4°C. On the next day, supernatant/antibody/bead mixtures were spun for 1 min at high speed and the beads were washed three times with RIPA buffer, then the proteins were eluted by incubating with 40 μl loading buffer containing β-mercaptoethanol for 30 min at RT and immunoblotted as described above with a mouse monoclonal antibody against the C-terminus of Cx32 (7C6.C7, diluted 1:10). Membranes were stripped by incubating in stripping buffer (100 mM β-mercaptoethanol, 2% SDS, and 62.5 mM Tris-HCl, pH 6.8) for 1 hr in 55°C, then reblotted with a rabbit antiserum against the C-terminal tail of Cx29 (Zymed; 1:1,000).

Recording From Transfected Mammalian Cell Lines

To identify transfected cells with fluorescence microscopy, Cx29, Cx32T²⁹, and Cx32L²⁹T²⁹ were subcloned into pIREs-EGFP2 (Clontech, Mountain View, CA); Cx32 was subcloned into pIREs-dsRed monomer, which was produced by replacing the coding sequencing of EGFP with that dsRed-monomer. Neuro2A cells were transiently transfected using Lipofectamine 2000 (Gibco Invitrogen) as described above, except that Lipofectamine 2000/DNA complexes were added to antibiotic-free media rather than Optimem. Dual whole-cell voltage clamping and analysis was performed as previously described (Abrams et al., 2003). Recording solutions were as follows: pipette solution, 145 mM CsCl, 5 mM EGTA, 0.5 mM CaCl₂, 10 mM HEPES, pH 7.2; bath solution, 150 mM NaCl, 4 mM KCl, 1 mM MgCl₂, 2 mM CaCl₂, 5 mM dextrose, 2 mM pyruvate, 10 mM HEPES, pH 7.4. Junctional conductances were determined from isolated pairs by measuring instantaneous junctional current responses to junctional voltage pulses from 0 to ±40 or ±100 mV and applying Ohm’s law. Cytoplasmic bridges were excluded by demonstrating the sensitivity of the junctional conductances to application of bath solution containing 2 mM octanol. Values are presented as mean ± SEM. Levels of coupling were compared using a Kruskal-Wallis test with Dunn’s multiple-comparisons test.

RESULTS

Cx29 Is Localized to the Cell Membrane but Does Not Form Functional Gap Junctions

To determine the cellular localization of mouse Cx29 (mCx29), we transiently transfected gap junction-deficient HeLa cells and immunostained them with an antiserum against the cytoplasmic C-terminus of Cx29 (Altevogt et al., 2002). About 50% of cells were Cx29 positive (Fig. 1A), whereas cells transfected with an “empty” expression plasmid or parental cells were not labeled (data not shown). There was Cx29 immunoreactivity throughout the cell membrane, including cellular processes, as shown directly by double staining cells for Cx29 and a “pan-cadherin” monoclonal antibody (Suppl. Fig. 1A). Although many cells showed continuous staining along apposed cell membranes for both Cx29 and cadherin, we did not find discrete puncta of Cx29 immunoreactivity at apposed cell borders, which are traditionally considered to be gap junction plaques. In contrast, transiently transfected cells that express Cx32 (Fig. 1E, Suppl. Fig. 1E), Cx26, Cx30, Cx43, or Cx47 (Orthmann-Murphy et al., 2007; Yum et al., 2007; and data not shown), had gap junction plaques on apposed cell membranes. We repeated these experiments more than 10 times and used at least two different antisera against Cx29 and Cx32, with similar results. Cx29 was similarly localized in bulk-selected HeLa cells that stably expressed Cx29 and did not appear to form gap junction plaques (Suppl. Fig. 2). We confirmed the localization of Cx29 and Cx32 in transfected COS-7 and Neuro2A cells (data not shown).

These data suggested that Cx29 does not form gap plaques, in accordance with the previously described lack of junctional conductance between transfected cells that express Cx29 (Altevogt et al., 2002). To confirm this, we “scrape loaded” confluent monolayers of cloned HeLa cells that stably expressed Cx29. In this assay (El-Fouly et al., 1987), cells are wounded with a razor or scalpel blade in the presence of Lucifer yellow (LY; 443 Da, -2 charge), which permeates homotypic Cx32 channels (Elfgang et al., 1995). LY did not spread beyond the wounded parental cells (not shown) or cells that stably express Cx29 (Fig. 2A), whereas LY spread several cell diameters in HeLa cells stably expressing Cx32 (Fig. 2E) or Cx47 (Orthmann-Murphy et al., 2007). This experiment was repeated three times, with similar results.

To demonstrate more directly that Cx29-expressing cells are not coupled by gap junctions, we performed FRAP. Confluent cultures of parental cells as well as cloned HeLa cells that stably expressed Cx29 or human Cx47 were incubated in calcein AM ester, which diffuses into cells and then is cleaved to release calcein, a fluorescent cytoplasmic dye (623 Da, -4). The fluorescence was measured in a small group of cells, which were then photobleached, and the measurements were repeated every 10 sec for 30 min (Fig. 3). Cells stably expressing Cx47 showed 50% recovery after about 5 min, whereas parental cells and cells stably expressing Cx29 recovered at a similar and much slower rate, to less than 10% of the original level even after 30 min. These data, taken together, confirm that Cx29 does not form functional intercellular channels.

Domain Swaps Between Cx29 and Cx32

To investigate why Cx29 does not form gap junction plaques, we generated a series of chimeric Cx29/Cx32 proteins, depicted in Figure 1, by exchanging the intracellular loops and/or the intracellular C-terminal tails, the most divergent parts of connexins (Willecke et al., 2002). Immunoblots of cell lysates from transiently transfected cells demonstrated that each construct was expressed, although the amounts of Cx32L²⁹ and Cx32L²⁹T²⁹ were consistently less than those of the other constructs in four separate experiments, one of which is shown in Figure 4.

To examine the localization of these chimerae, cells were immunostained with well-characterized antibodies against the C-terminus of Cx29 (Cx29T), the intracellular loop of Cx32 (Cx32L), and/or the C-terminus of Cx32 (Cx32T); examples are shown in Figure 1 and

Supplemental Figure 1. Certain chimerae could be immunostained with a mouse monoclonal and a rabbit antiserum against two different regions; in every case, both antibodies gave the identical pattern of staining (Suppl. Fig. 3). We performed this analysis in at least 10 separate experiments on transiently transfected cells and also on bulk-selected cells that stably expressed these constructs (data not shown), with similar results. Similar to cells expressing Cx29, cells expressing Cx29L³², Cx29T³², or Cx29L³²T³² had diffuse membrane staining of the chimeric proteins and no gap junction plaques; this can best be seen by comparing their localization with that of cadherins (Suppl. Fig. 1).

In contrast to chimerae with a Cx29 backbone, those with a Cx32 backbone had little cell surface expression. Cx32L²⁹ had a diffuse, intracellular pattern of staining (Fig. 1F, Suppl. Fig. 1F), appearing similar to the endoplasmic reticulum (ER); this was confirmed by double-labeling with the ER protein GRP94 (Suppl. Fig. 4). Cx32T²⁹ and Cx32L²⁹T²⁹, like Cx32 itself, were prominently localized to intracellular puncta (Fig. 1, Suppl. Figs. 1, 3). For Cx32T²⁹, Cx32L²⁹T²⁹, and Cx32, we confirmed that at least some of the intracellular puncta were in endosomes, by double labeling with the rabbit antiserum against Cx29T and a goat antiserum against the late endosomal marker Rab7 (Suppl. Fig. 5). A quantitative analysis of pixel overlap demonstrated that a greater proportion of Cx32T²⁹, Cx32L²⁹T²⁹, and Cx32 immunoreactivity was colocalized with Rab7 than for cells expressing Cx29 (Table I).

To corroborate the apparent cell surface expression, we biotinylated cell membrane proteins of transiently transfected cells with a membrane-impermeant reagent. The biotinylated proteins were isolated using an avidin column, and the “bound” proteins were compared with the “unbound” proteins by immunoblotting as shown in Figure 5. There was a clear signal in the avidin-bound samples (and unbound samples) from cells expressing Cx29, Cx32, Cx29L³², Cx29T³², and Cx29L³²T³² or Cx32T²⁹. As in the immunoblot (Fig. 4), the signals in the bound and unbound fractions for Cx32L²⁹T²⁹ were much weaker. No signal was detected for Cx32L²⁹, consistent with the finding that this chimera is localized in the ER and hence not accessible to the biotinylation reagents. Among the proteins that reach the cell membrane, Cx32 had the lowest bound/unbound ratio, perhaps because gap junction plaques were less accessible to the biotinylation reagent. Reprobing the blot for actin demonstrated that intracellular proteins did not contaminate the avidin-bound fraction. This experiment was repeated three times with similar results. These data indicate that all of the chimerae except for Cx32L²⁹ appear to reach the cell membrane after transient transfection.

Because the ability to form functional gap junctions is thought to depend on the compatibility of the extracellular loops of apposed connexin molecules, it was surprising that the Cx32L²⁹, Cx32T²⁹, and Cx32L²⁹T²⁹ chimerae failed to form gap junction plaques. To investigate this issue further, we utilized dual whole-cell patch clamp recordings to study the ability of the these chimerae to form channel both in the homotypic configuration and when paired heterotypically with wild-type (WT) mouse Cx32. In contrast to homotypic WT Cx32 controls, none of the cell pairs was electrically coupled above the levels observed in untransfected pairs of Neuro2A (Table II).

Cx32 and Cx29 Do Not Directly Interact

To evaluate further the possibility that Cx32 and Cx29 directly interact, we performed coimmunoprecipitations of transiently transfected HeLa cells. In pilot experiments, immunoprecipitation with a rabbit antiserum against the C-terminus of Cx29, followed by immunoblotting with a mouse monoclonal antibody against the C-terminus of Cx32, proved to be the only effective combination. As shown in Figure 6 (lane 3), Cx32 did not appear to coimmunoprecipitate with Cx29. Reprobing the same blot demonstrated that Cx29 was present in the appropriate samples. This experiment was repeated four times, with similar results. Immunostaining transiently transfected cells that expressed both Cx32 and Cx29 showed that

the patterns of Cx32 and Cx29 immunoreactivity appeared similar to the pattern in cells that had been transfected with either plasmid alone (Fig. 7A). Although some overlap is evident, as might be expected by chance, the two connexins were not strongly colocalized. In contrast, Cx32 and Cx30 were completely colocalized in cotransfected cells (Yum et al., 2007). These data indicate that Cx32 and Cx29 do not directly interact, at least in transfected cells.

The Intracellular Loop of Cx29 Facilitates Homomeric Interactions

We also used coimmunoprecipitations to determine which domains of Cx29 and Cx32 facilitate homomeric interactions (between Cx29 and Cx29 or Cx32 and Cx32). As described above, cells were cotransfected, and lysates were immunoprecipitated with the rabbit antiserum against Cx29T, followed by immunoblotting with the monoclonal antibody against Cx32T. With this strategy, we could evaluate three of six possible combinations for Cx29 (Cx29 and Cx29T³², Cx29L³²T³², or Cx32L²⁹ but not Cx29L³², Cx32T²⁹, or Cx32L²⁹T²⁹) and three of six possible combinations for Cx32 (Cx32 and Cx29L³², Cx32T²⁹, Cx32L²⁹T²⁹ but not Cx29T³², Cx29L³²T³², or Cx32L³²). This experiment was repeated four times with similar results, one of which is shown in Figure 6. Cx32T²⁹ (lane 6) and Cx32L²⁹T²⁹ (lane 9) coimmunoprecipitated Cx32, indicating that homomeric interactions of Cx32 do not require either the Cx32 loop or the Cx32 tail. Cx29L³² did not coimmunoprecipitate Cx32 (lane 18), indicating that the Cx32 loop was not sufficient for homomeric interactions with WT Cx32. In contrast, Cx29 coimmunoprecipitated Cx29T³² (lane 12) much more robustly than Cx29L³²T³² (lane 15), and even coimmunoprecipitated Cx32L²⁹ (lane 21), indicating that the Cx29 loop is sufficient for homomeric interactions. Thus, for Cx32, homomeric interactions mostly involve regions other than the intracellular loop or the C-terminus–N-terminus, transmembrane domains, and extracellular loops. For Cx29, the loop domain is sufficient for homomeric interactions, although other domains likely participate.

We also immunostained cells that were transfected with the same combinations of constructs used in the coimmunoprecipitation analysis. Cx29 and Cx29T³² (Fig. 7B) as well as Cx29 and Cx29L³²T³² (Fig. 7C) were colocalized throughout the cell membrane. Cx32 and Cx32T²⁹ (Fig. 7E) as well as Cx32 and Cx32L²⁹T²⁹ (Fig. 7F) were colocalized in intracellular puncta, but not in gap junction plaques, indicating that Cx32 did not “mislocalize” Cx32T²⁹ or Cx32L²⁹T²⁹ to gap junction plaques. Similarly, Cx29 and Cx32L²⁹ may be partially colocalized in the ER but not in the cell membrane, indicating that Cx29 does not “mislocalize” Cx32L²⁹ to the cell membrane. Cx32 and Cx29L³² did not appear to be colocalized (Fig. 7G). These experiments were performed three times, with similar results. Thus, with the possible exception of Cx29 and Cx32L²⁹, pairs of connexins that were coimmunoprecipitated also appeared to be colocalized, but this did not enable chimerae to form gap junction plaques (Cx32T²⁹ or Cx32L²⁹T²⁹) or even to reach the cell membrane (Cx32L²⁹).

DISCUSSION

Cx29 Does Not Form Functional Gap Junctions

Our findings that Cx29 is efficiently incorporated into the cell membranes of transfected cells but does not form gap junction plaques or functional gap junctions that pass LY or calcein extend our earlier result showing that cells expressing Cx29 do not form functional channels with cells expressing either Cx29 or Cx32 (Altevogt et al., 2002). In that paper, we also reported that cells coexpressing Cx29 and Cx32, however, could form channels with cells coexpressing Cx29 and Cx32 or with cells expressing Cx32 alone. We inferred that these channels were not homotypic Cx32 channels because the whole-cell conductances were asymmetric, and the single-channel conductances were prolonged and had novel substates compared with cells expressing Cx32 alone. The new data showing that Cx29 and Cx32 are not colocalized or coimmunoprecipitated indicate that they do not interact directly. It is difficult to reconcile these

two sets of findings; one possibility is that the electrophysiological assay in our prior study is more sensitive than the immunological assays used here.

Unlike Cx29, most connexins can form functional homotypic channels, including Cx30.2, which can also form hemichannels (Kreuzberg et al., 2005; Bukauskas et al., 2006). Cx29 also differs from Cx30.3 and Cx33, which do not efficiently traffic to the cell membrane or form functional gap junctions when expressed alone by transfection but can interact with other connexins. Cx30.3 forms heteromeric functional gap junctions when coexpressed with Cx31, as shown by their colocalization and coimmunoprecipitation (Plantard et al., 2003); these two connexins likely form heteromeric Cx30.3/Cx31 channels in keratinocytes (Richard et al., 2003). In transfected cells, Cx33 inhibits Cx43 from forming gap junction plaques and functional gap junctions (Chang et al., 1996; Fiorini et al., 2004), but perhaps not *in vivo* (Tan et al., 1996).

Cx29/Cx32 Chimerae Do Not Form Functional Channels

We investigated swapped domains of Cx29 and Cx32, thereby potentially illuminating the molecular basis of their divergent behaviors. Such domain swaps have been performed many times, mostly to illuminate the structural basis of the biophysical differences between connexin channels and hemichannels (Rubin et al., 1992; Haubrich et al., 1996; Wang et al., 1996; Trexler et al., 2000; Maza et al., 2005; Dong et al., 2006; Hu et al., 2006); there have been few reports on heteromeric or heterotypic compatibility. White et al. (1995) made a mouse Cx32/Cx43 chimera starting at the beginning of the intracellular loop, and found that this chimera could form channels with other connexins in Cx43-like manner, thus implicating the second extracellular loop as the prime mediator of heterotypic (connexon-connexon) compatibility. The importance of the extracellular loops in determining the heterotypic compatibility between Cx40 and Cx43 was confirmed by Haubrich et al. (1996), who found that the cytoplasmic loop and the C-terminus may contribute, too. Manthey et al. (2001) exchanged the intracellular loop and/or the C-termini of mouse Cx26 and Cx30, which are the most closely related connexins, but differ in that intercellular channels composed of Cx30 do not pass LY in transfected cells (cf. Beltramello et al., 2003). They ascribed this difference to the combined actions of the loop and C-terminus, because Cx30L²⁶T²⁶, but neither Cx30L²⁶ nor Cx30T²⁶, showed transfer of LY. Conversely, Cx26L³⁰ and Cx26T³⁰ appeared permeable to LY, but Cx26L³⁰T³⁰ did not. These findings are in accordance with the idea that interactions between the intracellular loop and the C-terminus are important determinants of channel function (Delmar et al., 2000, 2004).

Our results depart from these earlier studies. First, altered trafficking of chimerae was not reported, although some studies relied on expression in *Xenopus* oocytes (Rubin et al., 1992; White et al., 1995), which may be more permissive than mammalian cells for allowing altered proteins to the cell membrane (Oh et al., 1997; Yum et al., 2002; Wang et al., 2004). In our studies, replacing the intracellular loop domain of Cx32 with that of Cx29 (Cx32L²⁹) resulted in localization in the ER, indicating that Cx32L²⁹ did not attain a properly folded conformation required for export from the ER (Leube, 1995; VanSlyke et al., 2000; Kleopa et al., 2002). Second, homomeric interactions of Cx29 also appeared to involve the intracellular loop, which has not been previously reported for other connexins. Third, even though Cx32T²⁹ and Cx32L²⁹T²⁹ have the extracellular loops of Cx32, they do not form gap junction-like plaques, indicating that the extracellular loops (E2 in particular) are not solely responsible for connexon-connexon interactions (White et al., 1995; Haubrich et al., 1996; Martin and Evans, 2004). These chimerae were expressed at the cell surface to a limited degree, but accumulated in endosomes, indicating that they were retrieved from the cell membrane and ultimately degraded by lysosomes (Laing et al., 1997; VanSlyke et al., 2000; Kleopa et al., 2002).

The suggestion that the C-terminus is required to form homotypic channels is contradicted by the prior finding that deleting most of the C-terminus does not prevent Cx32 from forming functional channels. Whereas the Tyr211stop and Cys217stop mutants do not reach the cell membrane, the Arg220stop mutant and most missense mutations affecting the C-terminus reach the cell membrane and form functional gap junctions, although most have abnormal biophysical properties (Castro et al., 1999; Abrams et al., 2000; Kleopa et al., 2002; Yum et al., 2002). Thus, substituting the intracellular loop and/or tail of Cx32 with those of Cx29 appears to prevent Cx32 from forming functional gap junctions.

Differential Targeting of Connexins

Understanding the molecular basis of the differences between Cx29 and Cx32 may elucidate the pathogenesis of demyelination in X-linked Charcot-Marie-Tooth disease, a common hereditary neuropathy caused by mutations in *GJB1*, the gene that encodes Cx32 (Kleopa and Scherer, 2006). Cx29 does not appear to “rescue” the phenotype of *cx32* null mice, even though both are coexpressed in myelinating glia, perhaps because Cx32, but not Cx29, can form functional gap junctions. Our finding that Cx29 and Cx32 do not appear to interact directly *in vitro* is consistent with their distinct localizations in PNS and CNS myelin sheaths. Cx29 (but not Cx32) is localized on the adaxonal membrane of myelinating Schwann cells and oligodendrocytes and does not appear to form gap junctions with the apposed axons but could form hemichannels (Goodenough and Paul, 2003). Furthermore, their localizations do not depend on each other, because Cx29 is normally localized in *cx32* null mice (Altevogt et al., 2002; Nagy et al., 2003b) and Cx32 is normally localized in *cx29* null mice (D. Paul, unpublished observations).

How Cx29 and Cx32 become localized in distinct aspects of cell membranes is unknown. For connexins that have a C-terminal PDZ binding domain (like Cx43 and Cx47), interaction with ZO-1 may mediate their localization (Giepmans and Moolenaar, 1998; Li et al., 2004; Hunter et al., 2005). Neither Cx29 nor Cx32, however, has a consensus PDZ binding domain. The distal C-terminus of Cx32 has a prenylation motif (CaaX), but this does not appear to be essential for its localization in myelinating Schwann cells (Huang et al., 2005). Perhaps interactions between Cx32 and other molecules such as Dlg1 (Duffy et al., 2007) mediate its localization. By using transgenic expression of the constructs that we have generated here, it should be possible to examine the localization of various chimeras in Cx29- and/or Cx32-deficient myelin sheaths, to determine whether the intracellular loop and/or C-terminus modifies their localization (Huang et al., 2005; Bone Jeng et al., 2006).

Supplementary Material

Refer to Web version on PubMed Central for supplementary material.

Acknowledgements

Contract grant sponsor: NIH; Contract grant number: NS42878 (to S.S.S.); Contract grant number: NS43560 (to S.S.S.).

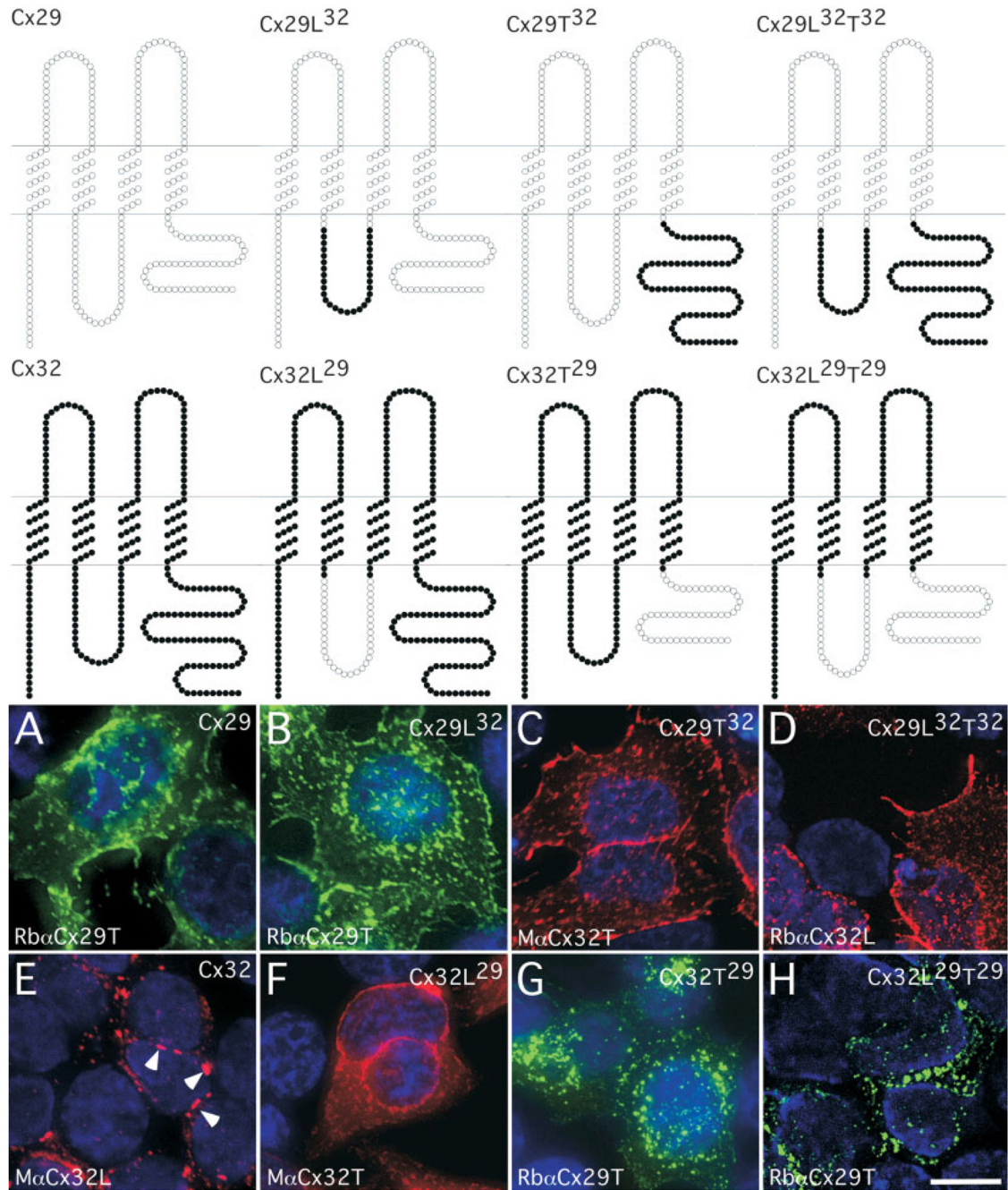
We thank Drs. Klaus Willecke and Bruce Nicholson for the HeLa cells; Dr. Elliot Hertzberg for antibodies; Dr. Edward Cooper for use of equipment; Michael Seminack for technical assistance; and Marion Scott, Ethan Hughes, and Drs. Patricio Meneses and Linda Musil for advice. NIH grant P30 NS047321 supports the University of Pennsylvania Dynamic Imaging Center, where the FRAP experiments were performed. Disclosure: P.G.H. has an equity interest in Prairie Technologies, Inc., which manufactures a microscope used in these studies.

References

- Abrams CK, Oh S, Ri Y, Bargiello TA. Mutations in connexin 32: the molecular and biophysical bases for the X-linked form of Charcot-Marie-Tooth disease. *Brain Res Rev* 2000;32:203–214. [PubMed: 10751671]
- Abrams CK, Freidin M, Bukauskas F, Dobrenis K, Bargiello TA, Verselis VK, Bennett MVL, Chen L, Sahen Z. Pathogenesis of X-linked Charcot-Marie-Tooth disease: differential effects of two mutations in connexin 32. *J Neurosci* 2003;23:10548–10558. [PubMed: 14627639]
- Altevogt BM, Kleopa KA, Postma FR, Scherer SS, Paul DL. Cx29 is uniquely distributed within myelinating glial cells of the central and peripheral nervous systems. *J Neurosci* 2002;22:6458–6470. [PubMed: 12151525]
- Beltramello M, Bicego M, Piazza V, Ciubotaru CD, Mammano F, D'Andrea P. Permeability and gating properties of human connexins 26 and 30 expressed in HeLa cells. *Biochem Biophys Res Commun* 2003;305:1024–1033. [PubMed: 12767933]
- Bone Jeng LJ, Messing A, Balice-Gordon R, Fischbeck KH, Scherer SS. The effects of a dominant connexin32 mutant in myelinating Schwann cells. *Mol Cell Neurosci* 2006;32:283–298. [PubMed: 16790356]
- Bruzzone R, White TW, Paul DL. Connections with connexins: the molecular basis of direct intercellular signaling. *Eur J Biochem* 1996;238:1–27. [PubMed: 8665925]
- Bukauskas FF, Kreuzberg MM, Rackauskas M, Bukauskienė A, Bennett MVL, Verselis VK, Willecke K. Properties of mouse connexin 30.2 and human connexin 31.9 hemichannels: Implications for atrioventricular conduction in the heart. *Proc Natl Acad Sci U S A* 2006;103:9726–9731. [PubMed: 16772377]
- Castro C, Gomez-Hernandez JM, Silander K, Barrio LC. Altered formation of hemichannels and gap junction channels caused by C-terminal connexin-32 mutations. *J Neurosci* 1999;19:3752–3760. [PubMed: 10234007]
- Chang M, Werner R, Dahl G. A role for an inhibitory connexin in testis? *Dev Biol* 1996;175:50–56. [PubMed: 8608868]
- Delmar, M.; Stergiopoulos, K.; Homma, N.; Calero, G.; Morley, G.; EkVitorin, JF.; Taffet, SM. A molecular model for the chemical regulation of connexin43 channels: the “ball-and-chain” hypothesis. In: Peracchia, C., editor. *Gap junctions*. San Diego: Academic Press Inc; 2000. p. 223–248.
- Delmar M, Coombs W, Sorgen P, Duffy HS, Taffet SA. Structural bases for the chemical regulation of connexin43 channels. *Cardiovasc Res* 2004;62:268–275. [PubMed: 15094347]
- Deschênes SM, Walcott JL, Wexler TL, Scherer SS, Fischbeck KH. Altered trafficking of mutant connexin32. *J Neurosci* 1997;17:9077–9084. [PubMed: 9364054]
- Dong L, Liu X, Li H, Vertel BM, Ebihara L. Role of the N-terminus in permeability of chicken connexin45.6 gap junctional channels. *J Physiol* 2006;576:787–799. [PubMed: 16931554]
- Duffy HS, Iacobas I, Hotchkiss K, HirstJensen BJ, Bosco A, Dandachi N, Dermietzel R, Sorgen PL, Spray DC. The gap junction protein connexin32 interacts with the Src homology 3/Hook domain of discs large homolog 1. *J Biol Chem* 2007;282:9789–9796. [PubMed: 17284442]
- Eiberger J, Kibschull M, Stvenzke N, Schober A, Bussov H, Wessig C, Djahed S, Reucher H, Koch DA, Lautermann J, Moser T, Winterhager E, Willecke K. Expression pattern and functional characterization of connexin29 in transgenic mice. *Glia* 2006;53:601–611. [PubMed: 16435366]
- El-Fouly M, Trosko J, Chang C. Scrape-loading and dye transfer. A rapid and simple technique to study gap junctional intercellular communication. *Exp Cell Res* 1987;168:422–430. [PubMed: 2433137]
- Elfang C, Eckert R, Lichtenberg-Frate H, Butterweck A, Traub O, Klein RA, Hulser DF, Willecke K. Specific permeability and selective formation of gap junction channels in connexin-transfected HeLa cells. *J Cell Biol* 1995;129:805–817. [PubMed: 7537274]
- Fiorini C, Mograbi B, Cronier L, Bourget I, Decrouy X, Nebout M, Ferrua B, Malassine A, Samson M, Fenichel P, Segretain D, Pointis G. Dominant negative effect of connexin33 on gap junctional communication is mediated by connexin43 sequestration. *J Cell Sci* 2004;117:4665–4672. [PubMed: 15331631]

- Giepmans BNG, Moolenaar WH. The gap junction protein connexin43 interacts with the second PDZ domain of the zona occludens-1 protein. *Curr Biol* 1998;8:931–934. [PubMed: 9707407]
- Goodenough DA, Paul DL. Beyond the gap: Functions of unpaired connexon channels. *Nat Rev Mol Cell Biol* 2003;4:285–294. [PubMed: 12671651]
- Haubrich S, Schwarz H-J, Bukauskas F, Lichtenberg-Frate H, Traub O, Weingart R, Willecke K. Incompatibility of connexin 40 and 43 hemichannels in gap junctions between mammalian cells is determined by intracellular domains. *Mol Biol Cell* 1996;7:1995–2006. [PubMed: 8970160]
- Hu XG, Ma MY, Dahl G. Conductance of connexin hemichannels segregates with the first transmembrane segment. *Biophys J* 2006;90:140–150. [PubMed: 16214855]
- Huang Y, Sirkowski EE, Stickney JT, Scherer SS. Prenylation-defective human connexin32 mutants are normally localized and function equivalently to wild type connexin32 in myelinating Schwann cells. *J Neurosci* 2005;25:7111–7120. [PubMed: 16079393]
- Hunter AW, Barker RJ, Zhu C, Gourdie RG. Zonula occludens-1 alters connexin43 gap junction size and organization by influencing channel accretion. *Mol Biol Cell* 2005;16:5686–5698. [PubMed: 16195341]
- Kamasawa N, Sik A, Morita M, Yasumura T, Davidson KGV, Nagy JI, Rash JE. Connexin-47 and connexin-32 in gap junctions of oligodendrocyte somata, myelin sheaths, paranodal loops and Schmidt-Lanterman incisures: Implications for ionic homeostasis and potassium siphoning. *Neuroscience* 2005;136:65–86. [PubMed: 16203097]
- Kleopa KA, Scherer SS. Molecular genetics of X-linked Charcot-Marie-Tooth disease. *Neuromol Med* 2006;8:107–122.
- Kleopa KA, Yum SW, Scherer SS. Cellular mechanisms of connexin32 mutations associated with CNS manifestations. *J Neurosci Res* 2002;68:522–534. [PubMed: 12111842]
- Kleopa KA, Orthmann JL, Enriquez A, Paul DL, Scherer SS. Unique distributions of the gap junction proteins connexin29, connexin32, and connexin47 in oligodendrocytes. *Glia* 2004;47:346–357. [PubMed: 15293232]
- Kreuzberg MM, Sohl GS, Kim JS, Verselis VK, Willecke K, Bukauskas FF. Functional properties of mouse connexin30.2 expressed in the conduction system of the heart. *Circ Res* 2005;96:1169–1177. [PubMed: 15879306]
- Laing JG, Tadros PN, Westphale EM, Beyer EC. Degradation of connexin43 gap junctions involves both the proteasome and the lysosome. *Exp Cell Res* 1997;236:482–492. [PubMed: 9367633]
- Leube RE. The topogenic fate of the polytopic transmembrane proteins, synaptophysin and connexin, is determined by their membrane-spanning domains. *J Cell Sci* 1995;108:883–894. [PubMed: 7622617]
- Li J, Habbes HW, Eiberger J, Willecke K, Dermietzel R, Meier C. Analysis of connexin expression during mouse Schwann cell development identifies connexin29 as a novel marker for the transition of neural crest to precursor cells. *Glia* 2007;55:93–103. [PubMed: 17024657]
- Li X, Ionescu AV, Lynn BD, Lu S, Kamasawa N, Morita M, Davidson KGV, Yasumura T, Rash JE, Nagy JI. Connexin47, connexin29 and connexin32 coexpression in oligodendrocytes and Cx47 association with zonula occludens-1 (ZO-1) in mouse brain. *Neuroscience* 2004;126:611–630. [PubMed: 15183511]
- Li X, Lynn BD, Olson C, Meier C, Davidson KGV, Yasumura T, Rash JE, Nagy JL. Connexin29 expression, immunocytochemistry and freeze-fracture replica immunogold labelling (FRIL) in sciatic nerve. *Eur J Neurosci* 2002;16:795–806. [PubMed: 12372015]
- Manthey D, Banach K, Desplantez T, Lee CG, Kozak CA, Traub O, Weingart R, Willecke K. Intracellular domains of mouse connexin26 and -30 affect diffusional and electrical properties of gap junction channels. *J Membrane Biol* 2001;181:137–148. [PubMed: 11420600]
- Martin PEM, Evans WH. Incorporation of connexins into plasma membranes and gap junctions. *Cardiovasc Res* 2004;62:378–387. [PubMed: 15094357]
- Maza J, Das Sarma J, Koval M. Defining a minimal motif required to prevent connexin oligomerization in the endoplasmic reticulum. *J Biol Chem* 2005;280:21115–21121. [PubMed: 15817491]
- Nagy JI, Ionescu AV, Lynn BD, Rash JE. Connexin29 and connexin32 at oligodendrocyte and astrocyte gap junctions and in myelin of the mouse central nervous system. *J Comp Neurol* 2003a;464:356–370. [PubMed: 12900929]

- Nagy JI, Ionescu AV, Lynn BD, Rash JE. Coupling of astrocyte connexins Cx26, Cx30, Cx43 to oligodendrocyte Cx29, Cx32, Cx47: Implications from normal and connexin32 knockout mice. *Glia* 2003;44:205–218. [PubMed: 14603462]
- Oh S, Ri Y, Bennett MVL, Trexler EB, Verselis VK, Bargiello TA. Changes in permeability caused by connexin 32 mutations underlie X-linked Charcot-Marie-Tooth disease. *Neuron* 1997;19:927–938. [PubMed: 9354338]
- Orthmann-Murphy JL, Enriquez AD, Abrams CK, Scherer SS. Loss-of-function GJA12/connexin47 mutations cause Pelizaeus-Merzbacher-like disease. *Mol Cell Neurosci* 2007;34:629–641. [PubMed: 17344063]
- Plantard L, Huber M, Macari F, Meda P, Hohl D. Molecular interaction of connexin 30.3 and connexin 31 suggests a dominant-negative mechanism associated with erythrokeratoderma variabilis. *Hum Mol Genet* 2003;12:3287–3294. [PubMed: 14583444]
- Richard G, Brown N, Rouan F, Vander Schroeff JG, Bijlsma E, Eichenfield LE, Sybert VP, Greer KE, Hogan P, Campanelli C, Compton JG, Bale SJ, DiGiovanna JJ, Uitto J. Genetic heterogeneity in erythrokeratoderma variabilis: Novel mutations in the connexin gene GJB4 (Cx30.3) and genotype-phenotype correlations. *J Invest Dermatol* 2003;120:601–609. [PubMed: 12648223]
- Rubin JB, Verselis VK, Bennett MVL, Bargiello TA. A domain substitution procedure and its use to analyze voltage dependence of homotypic gap junctions formed by connexins 26 and 32. *Proc Natl Acad Sci U S A* 1992;89:3820–3824. [PubMed: 1315041]
- Scherer SS, Deschênes SM, Xu Y-T, Grinspan JB, Fischbeck KH, Paul DL. Connexin32 is a myelin-related protein in the PNS and CNS. *J Neurosci* 1995;15:8281–8294. [PubMed: 8613761]
- Tan IP, Roy C, Saez JC, Saez CG, Paul DL, Risley MS. Regulated assembly of connexin33 and connexin43 into rat Sertoli cell gap junctions. *Biol Reprod* 1996;54:1300–1310. [PubMed: 8724358]
- Tang WX, Zhang YP, Chang Q, Ahmad S, Dahlke I, Yi H, Chen P, Paul DL, Lin X. Connexin29 is highly expressed in cochlear Schwann cells, and it is required for the normal development and function of the auditory nerve of mice. *J Neurosci* 2006;26:1991–1999. [PubMed: 16481432]
- Trexler EB, Bukauskas FF, Kronengold J, Bargiello TA, Verselis VK. The first extracellular loop domain is a major determinant of charge selectivity in connexin46 channels. *Biophys J* 2000;79:3036–3051. [PubMed: 11106610]
- VanSlyke JK, Deschênes SM, Musil LS. Intracellular transport, assembly, and degradation of wild-type and disease-linked mutant gap junction proteins. *Mol Biol Cell* 2000;11:1933–1946. [PubMed: 10848620]
- Wang H-L, Chang W-T, Yeh T-H, Wu T, Chen M-S, Wu C-Y. Functional analysis of mutant connexin-32 associated with X-linked dominant Charcot-Marie-Tooth disease. *Neurobiol Dis* 2004;15:361–370. [PubMed: 15006706]
- Wang XG, Peracchia L, Peracchia C. Chimeric evidence for a role of the connexin cytoplasmic loop in gap junction channel gating. *Pflugers Arch* 1996;431:844–852. [PubMed: 8927500]
- White TW, Paul DL, Goodenough DA, Bruzzone R. Functional analysis of selective interactions among rodent connexins. *Mol Biol Cell* 1995;6:459–470. [PubMed: 7542941]
- Willecke K, Eiberger J, Degen J, Eckardt D, Romualdi A, Guldenagel M, Deutsch U, Söhl G. Structural and functional diversity of connexin genes in the mouse and human genome. *Biol Chem* 2002;383:725–737. [PubMed: 12108537]
- Yum SW, Kleopa KA, Shumas S, Scherer SS. Diverse trafficking abnormalities for connexin32 mutants causing CMTX. *Neurobiol Dis* 2002;11:43–52. [PubMed: 12460545]
- Yum SW, Zhang J-x, Vallunas V, Brink PR, White TL, Scherer SS. Human connexin26 and connexin30 form functional heteromeric and heterotypic channels. *Am J Physiol C* 2007;293:1032–1048.

**Fig. 1.**

Localization of Cx29, Cx32, and Cx29/Cx32 chimerae. The upper panels depict the structures of mouse Cx29, mouse Cx32, and the Cx29/Cx32 chimerae in which the cytoplasmic loop (L) and/or C-terminus (T) were exchanged. A–H are deconvolved images of transiently transfected HeLa cells that express the indicated construct, immunostained with a rabbit antiserum against the C-terminus of Cx29 (RbαCx29T; Altevogt et al., 2002) or Cx32 (RbαCx32T; Chemicon) or monoclonal antibodies against the intracellular loop (MαCx32L; Zymed) or C-terminus (MαCx32T; 7C6.C7) of Cx32 as indicated, and counterstained with DAPI (blue). Cx29 (A), Cx29L³² (B), Cx29T³² (C), and Cx29L³²T³² (D) are localized to the cell membrane, Cx32 (E) is localized to gap junction plaques (arrowheads) between apposed

cell membranes; Cx32L²⁹ (**F**) shows diffuse intracellular staining, and Cx32T²⁹ (**G**) and Cx32L²⁹T²⁹ (**H**) are found mostly in intracellular puncta. Scale bar = 10 μ m.

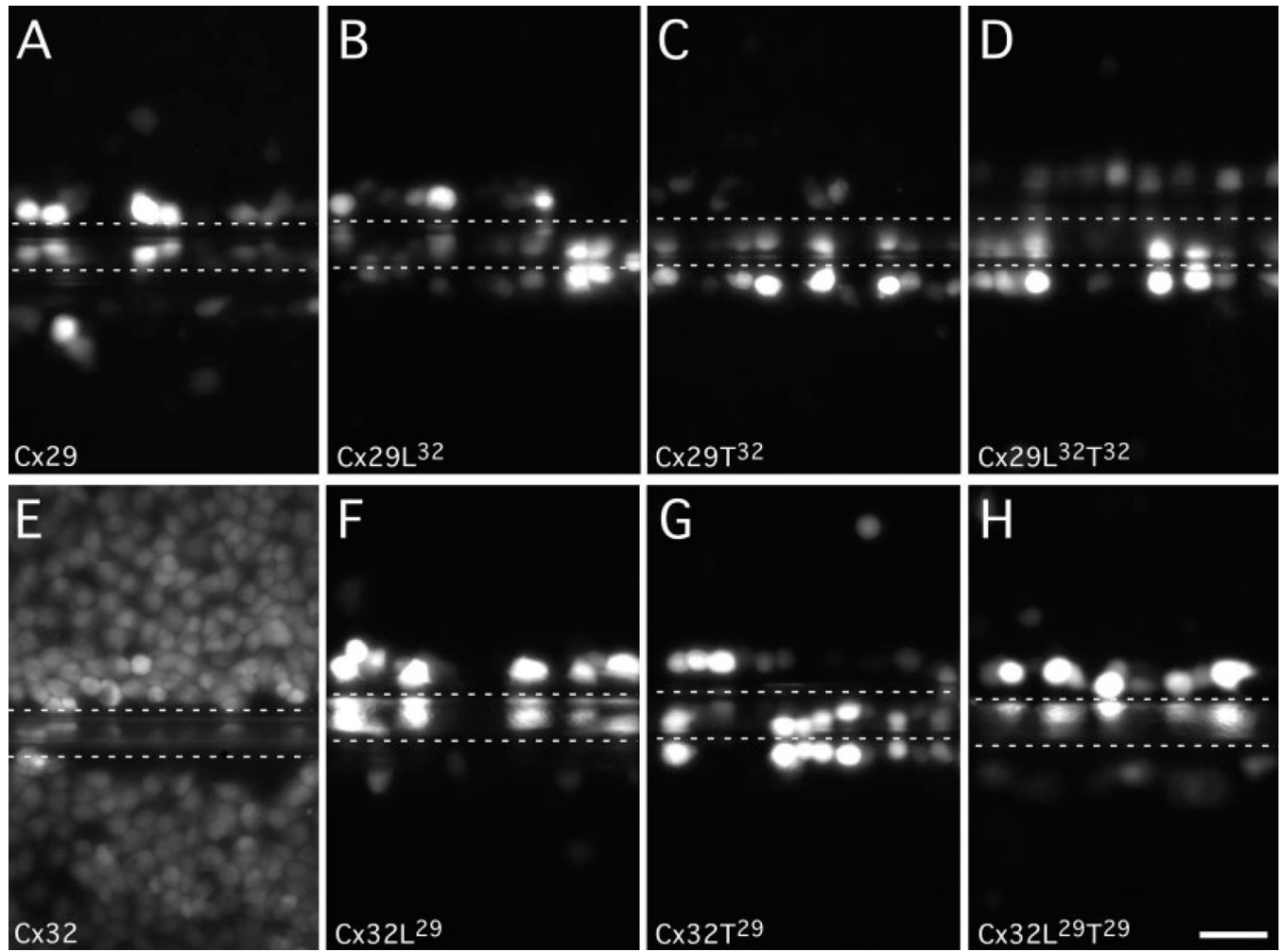
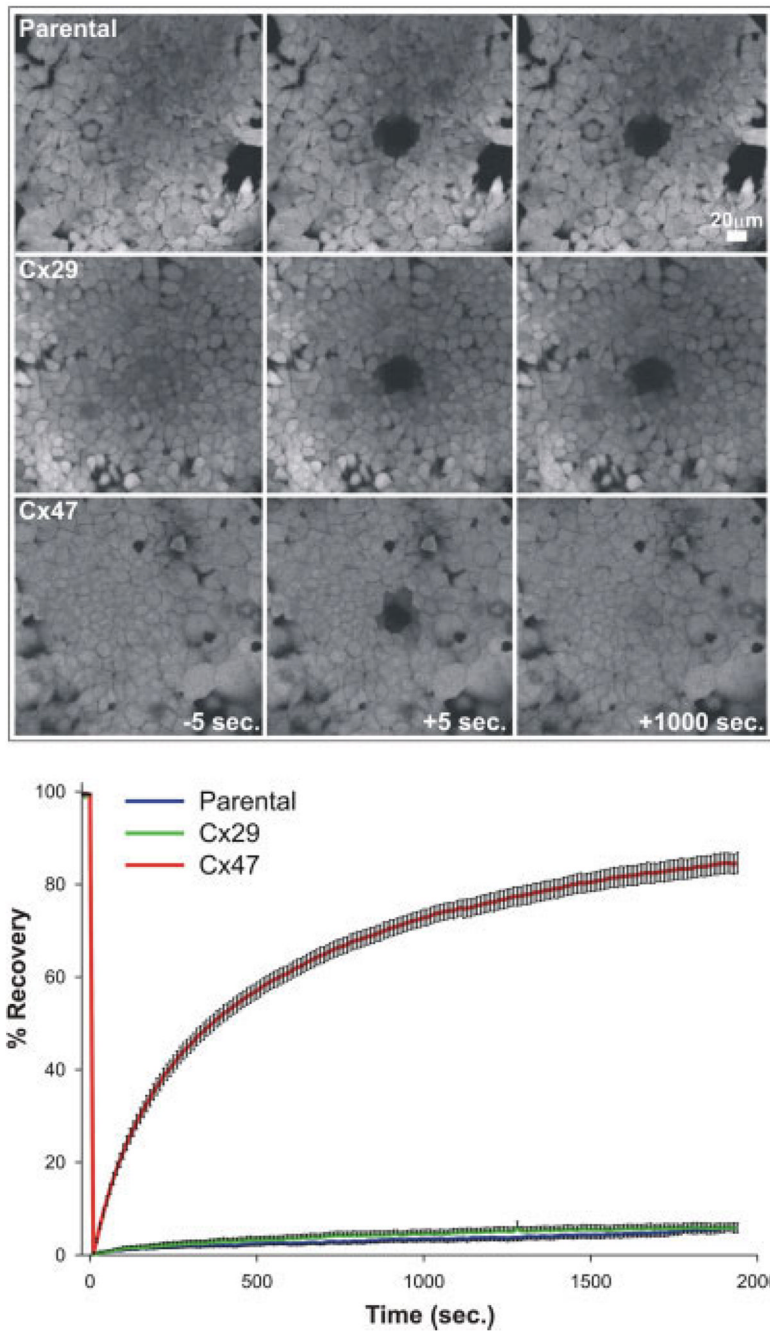


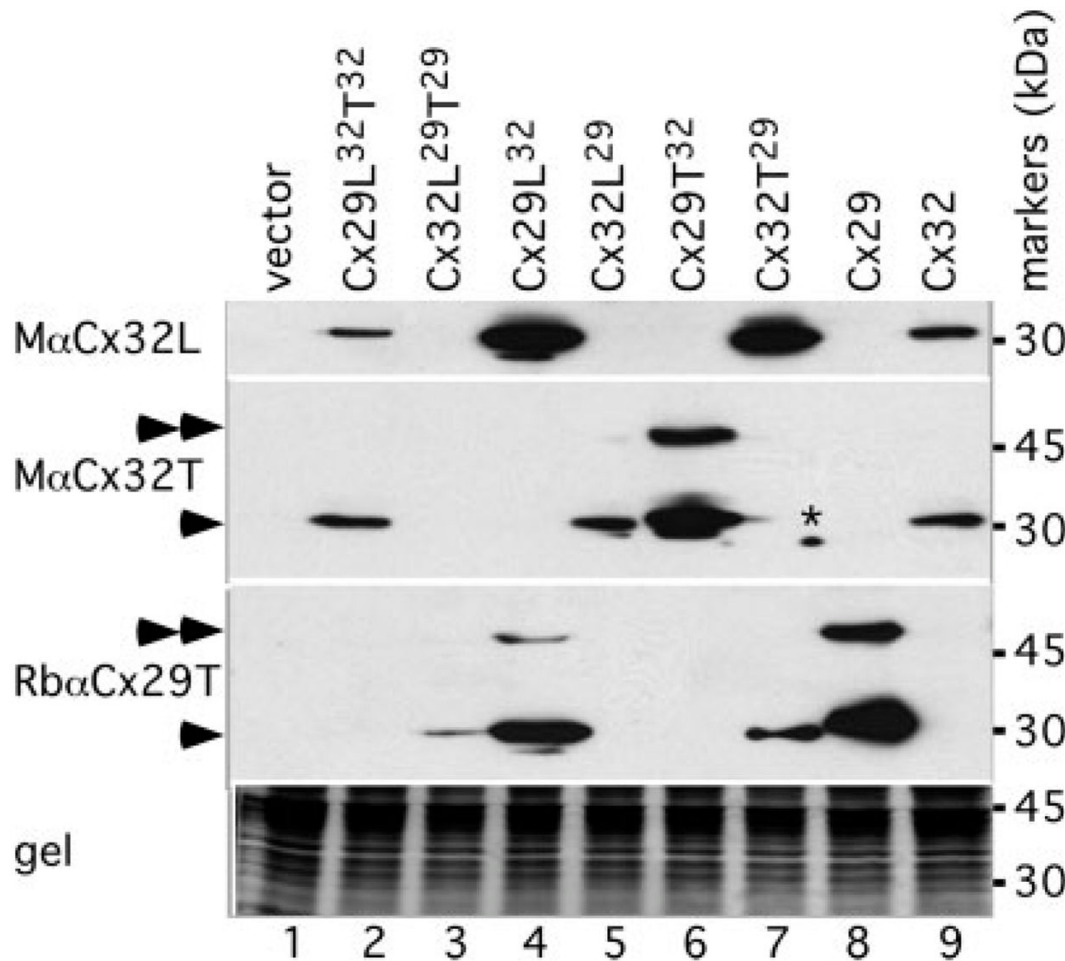
Fig. 2.

A–H: Cx29 or Cx29/Cx32 chimerae do not form functional gap junctions. These are digital images of scrape-loaded, confluent plates of bulk-selected HeLa cells that stably express the indicated constructs. The cells were incubated in 1% LY and imaged 5 min after injury with fluorescence optics to visualize LY. In cells expressing Cx32, LY diffuses into adjacent cells, whereas, in cells expressing Cx29 or one of the chimeric constructs, LY only labeled injured cells. Scale bar = 20 μ m.

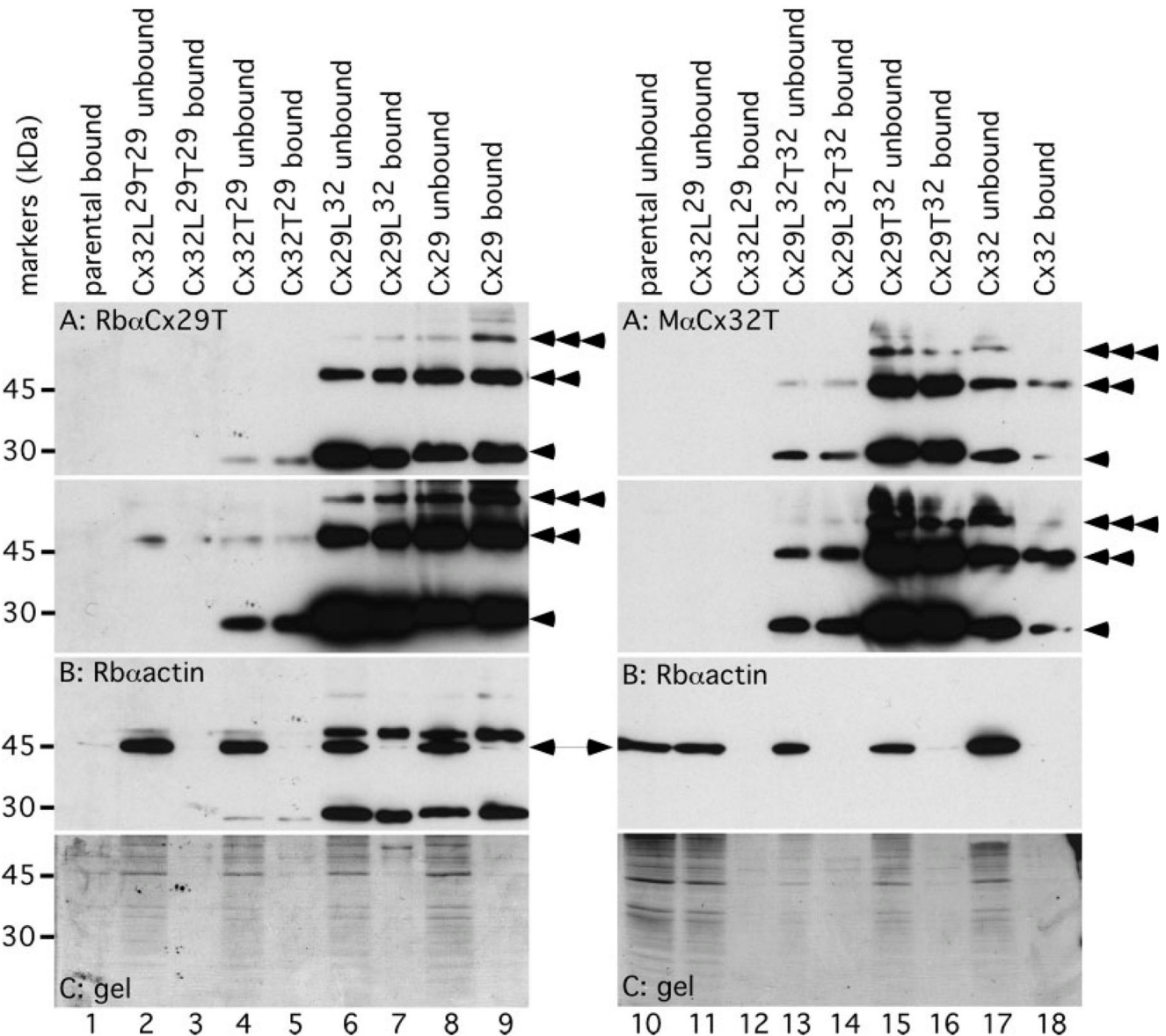
**Fig. 3.**

FRAP analysis of HeLa cells that stably express Cx29. The upper panels are digital images of parental HeLa cells or cloned HeLa cells that stably express mouse Cx29 or human Cx47. The cells were preloaded with calcein, and a small group of cells in the middle of the image was photobleached. Images are shown from cells 5 sec before (-5 sec) and 5 sec (+5 sec) and 1,000 sec (+1,000 sec) after photobleaching. The lower panel is a quantitative analysis of FRAP. Fluorescence was measured in the bleached area every 10 sec for 30 min. For every experiment, the measured region was considered to be 100% prior to bleaching, and 0% immediately following bleaching. Note the recovery of fluorescence in cells that express Cx47, but not in parental cells or in cells that express Cx29. The error bars show SEM, which is too small to be

illustrated for many samples. The number of imaged fields is as follows: HeLa cells ($n = 8$); HeLa cells that stably express mouse Cx29 ($n = 11$); HeLa cells that stably express human Cx47 ($n = 11$). Scale bar = 20 μm .

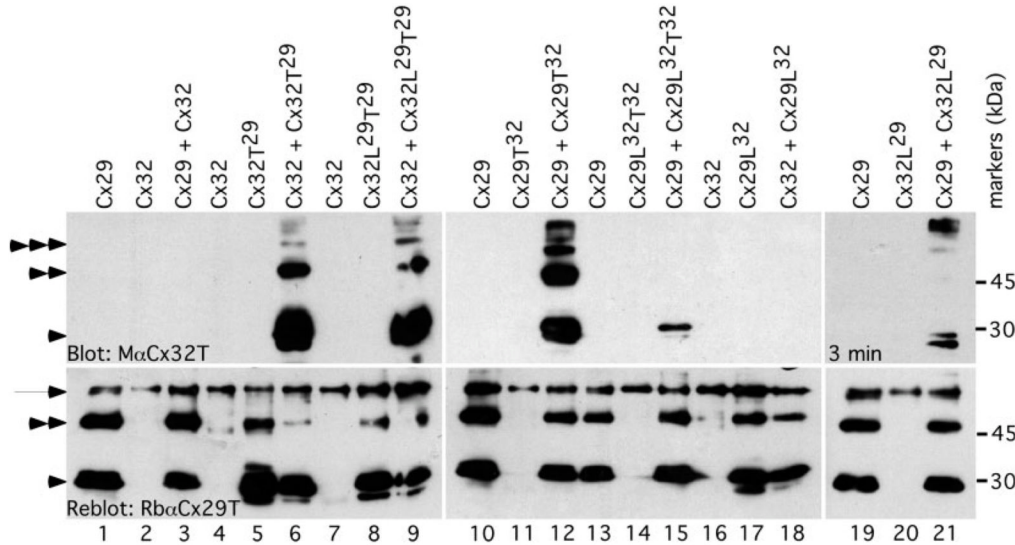
**Fig. 4.**

Immunoblot analysis of Cx29, Cx32, and Cx29/Cx32 chimerae. These are immunoblots of three identical membranes from lysates of HeLa cells that were transiently transfected with the indicated constructs; 80 μ g of each sample were separated by SDS-PAGE, transferred to a membrane, and probed with mouse monoclonal antibodies against the intracellular loop (Cx32L; Zymed) or Cterminus (Cx32T; 7C6.C7) of Cx32, or a rabbit antiserum against the C-terminus of Cx29 (Cx29T; Zymed). The membranes were incubated with peroxidase-conjugated donkey antibodies against mouse or rabbit IgG and developed with ECL. Although the intensities of the bands vary for each construct, Cx32L²⁹ (lane 5) and Cx32L²⁹T²⁹ (lane 3) being the lightest, monomers (arrowheads) of the appropriate size are detected with the appropriate antibodies; the higher molecular mass bands in some lanes are dimers (double arrowheads). The asterisk marks a spurious spot in the Cx32T²⁹ sample (lane 7). The image of the Coomassie-stained gel is shown to document equal loading of the samples.

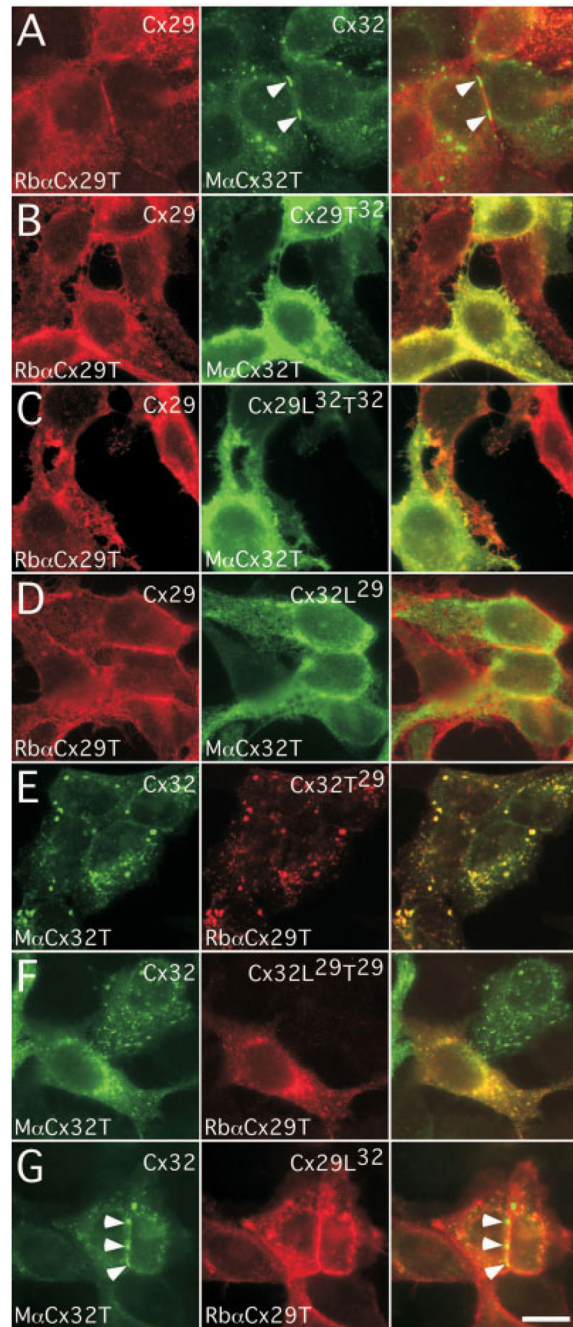
**Fig. 5.**

Cx29, Cx32, and some Cx29/Cx32 chimerae reach the cell membrane. HeLa cells were transiently transfected with the indicated constructs, then biotinylated, washed, and lysed. The lysates were incubated with avidin beads, and the avidin-bound fractions and 25 μ l of unbound fractions were separated on SDS-PAGE gels and transferred to two membranes, which were hybridized with either a rabbit antiserum against the C-terminus of Cx29 (Cx29T; Zymed) or a mouse monoclonal antibody against the C-terminus of Cx32 (Cx32T; Cx32T). The membranes were incubated with peroxidase-conjugated donkey antibodies against rabbit or mouse IgG and developed with ECL. **A:** Two exposure times are shown; monomer (arrowhead), dimers (double arrowhead), and trimers (triple arrowheads) are seen in the bound (and unbound) fraction from biotinylated cells that express Cx29 (lane 9), Cx32 (lane 18), Cx29L³² (lane 7), Cx29T³² (lane 16), and Cx29L³²T³² (lane 14). Weaker signal is detected in the bound and unbound fractions for Cx32T²⁹ (lane 5) and Cx32L²⁹T²⁹ (lane 3), and no signal is detected for Cx32L²⁹ (lane 12). **B:** The membranes were stripped and reprobed with a rabbit

antiserum against actin. Note that all unbound fractions contain a more robust actin signal (arrows) than do their corresponding bound samples, demonstrating that intracellular proteins were not biotinylated. The other bands in the left image result from the incompletely stripping of the rabbit antiserum against Cx29 C-terminus. The images of the Coomassie-stained gels document the loading of the samples (**C**).

**Fig. 6.**

Coimmunoprecipitation of Cx29, Cx32, and selected chimerae. Cells cotransfected with the indicated constructs and lysates were immunoprecipitated with a rabbit antiserum against the C-terminus of Cx29 (Zymed), the immunoprecipitates were separated on three gels, transferred to membranes, which were hybridized together with a mouse monoclonal antibody against the C-terminus of Cx32 (Cx32T; 7C6.C7) and developed with ECL. The blots were rehybridized together with an antiserum against the C-terminus of Cx29 (Cx29T; Zymed) and developed with ECL. In each row, the film was exposed for the same amount of time, except for top right panel, which was exposed longer (3 min). Note that Cx32 is not coimmunoprecipitated with Cx29 (lane 3); that replacing the C-terminus (Cx32T²⁹; lane 6) or even the C-terminus and the intracellular loop of Cx32 (Cx32L²⁹T²⁹; lane 9) with those of Cx29 does not prevent the coimmunoprecipitation with Cx32; that replacing the C-terminus and the intracellular loop of Cx29 (Cx29L³²T³²; lane 15) with those of Cx32 diminished the coimmunoprecipitation, with Cx29 more than replacing the C-terminus alone (Cx29T³²; lane 12). Furthermore, replacing the intracellular loop of Cx32 with that of Cx29 (Cx32L²⁹) promotes an interaction with Cx29 (lane 21), whereas replacing the intracellular loop of Cx29 with that of Cx32 (Cx29L³²) does not promote an interaction with Cx32 (lane 18). The arrow marks a spurious band that is present in all samples in the lower panels. The single, double, and triple arrowheads indicate the positions of connexin monomers, dimers, and multimers, respectively.

**Fig. 7.**

Localization of Cx29, Cx32, and various chimeras in transfected cells. These are images of HeLa cells that were transiently transfected to coexpress the indicated constructs and immunostained with a rabbit antiserum against the C-terminus of Cx29 (Cx29T; Altevogt et al. 2002) and a monoclonal antibody against the C-terminus of Cx32 (Cx32T; 7C6.C7). Note that Cx32 forms gap junction plaques (arrowheads), but neither Cx32 nor Cx29 (**A**) nor Cx32 and Cx29L³² (**G**) appear to be colocalized; that Cx29 and Cx29T³² (**B**) as well as Cx29 and Cx29L³²T³² (**C**) are colocalized throughout the cell membrane; that the Cx29 that is localized to the cell membrane does not “mislocalize” Cx32L²⁹, which is localized in the ER (**D**); and

that Cx32 and Cx32T²⁹ (**E**) as well as Cx32 and Cx32L²⁹T²⁹ (**F**) are colocalized in intracellular puncta. Scale bar ~10 μm.

TABLE IPixel Overlap of Rab7 and Cx32L²⁹T²⁹, Cx32T²⁹, Cx32, or Cx29*

	n	Percentage overlap of Cx pixels with Rab7 ¹	Percentage overlap of Rab7 pixels with Cx ²	Percentage overlap total pixels ³	Significance vs. Cx29
Cx32L ²⁹ T ²⁹	29	20.8 ± 6.27	38.4 ± 13.5	2.42 ± 0.85	<0.001
Cx32T ²⁹	18	24.9 ± 8.76	48.4 ± 16.9	3.05 ± 1.08	<0.001
Cx32	23	25.9 ± 7.11	46.8 ± 17.8	2.94 ± 1.11	<0.001
Cx29	25	13.3 ± 4.21	15.3 ± 6.94	0.97 ± 0.44	NA

*Transiently transfected cells expressing Cx32L²⁹T²⁹, Cx32T²⁹, Cx32, or Cx29 were immunostained for Rab7 and Cx29 (Cx32L²⁹T²⁹, Cx32T²⁹, Cx29) or Cx32 (Cx32) and imaged by confocal microscopy. For each cell, the brightest pixels in the Rab7 channel (6.0–6.5% of the total pixels) and Cx29/Cx32 channel (12.0–12.5% of the total pixels) were selected and used to determine the percentage overlap of selected pixels. For all comparisons, the pixel overlap was significantly higher between Rab7 and Cx29/Cx32 in cells expressing Cx32L²⁹T²⁹, Cx32T²⁹, or Cx32 than for cells expressing Cx29 (Mann-Whitney-Wilcoxon pairwise test).

¹The percentage of selected connexin pixels that overlap with the selected Rab7 pixels.

²The percentage of selected Rab7 pixels that overlap with the selected Cx pixels.

³The percentage of cell area is occupied by overlapping Rab7 and Cx pixels.

TABLE II

Dual Whole-Cell Patch Clamp Recordings*

	WT 32/WT 32	32L ²⁹ /32L ²⁹	32T ²⁹ /32T ²⁹	32L ²⁹ T ²⁹ /32L ²⁹ T ²⁹	32L ²⁹	32T ²⁹ /WT 32	32L ²⁹ T ²⁹ /WT 32
n	6	7	5	4	5	9	10
Mean (nS)	7.6	0.005	0.037	0	0	0	0.003
SEM	1.6	0.005	0.029	0	0	0	0.003
P	<0.001	<0.05	<0.001	<0.001	<0.001	<0.001	<0.001

*Neuro2A cells were transiently transfected to express the indicated construct and paired as shown, and gap junction coupling was measured (in nS). Cx32L²⁹, Cx32T²⁹, and Cx32T²⁹ chimerae did not form functional gap junctions when paired either homotypically (Cx32L²⁹/Cx32L²⁹, Cx32T²⁹/Cx32T²⁹, Cx32L²⁹T²⁹/Cx32L²⁹T²⁹) or heterotypically (with WT Cx32) above the levels observed in untransfected pairs of Neuro2A cells (which express rare endogenous channels (Orthmann-Murphy et al. 2007). The coupling in each of these cell pairs was significantly lower than that of WT Cx32/WT Cx32 homotypic pairs, which were well coupled.